

A Reversible Data Hiding Method in Compressible Encrypted Images

Shoko IMAIZUMI^{†a)}, Member, Yusuke IZAWA^{††}, Ryoichi HIRASAWA^{††}, Nonmembers,
and Hitoshi KIYA^{†††b)}, Fellow

SUMMARY We propose a reversible data hiding (RDH) method in compressible encrypted images called the encryption-then-compression (EtC) images. The proposed method allows us to not only embed a payload in encrypted images but also compress the encrypted images containing the payload. In addition, the proposed RDH method can be applied to both plain images and encrypted ones, and the payload can be extracted flexibly in the encrypted domain or from the decrypted images. Various RDH methods have been studied in the encrypted domain, but they are not considered to be two-domain data hiding, and the resultant images cannot be compressed by using image coding standards, such as JPEG-LS and JPEG 2000. In our experiment, the proposed method shows high performance in terms of lossless compression efficiency by using JPEG-LS and JPEG 2000, data hiding capacity, and marked image quality.

key words: Reversible data hiding, compressible encryption, image histogram, image retrieval

1. Introduction

Reversible data hiding (RDH) can perfectly retrieve original images from the marked images. It is particularly useful for medical, military, evidential images, and so forth [1–4]. For secure sharing of secret images, the image owner may encrypt the images beforehand. Here, we assume that some images are encrypted to protect their visual information. A third party, such as the system/channel administrator, may append additional information to the encrypted images. The image user hopes to restore the high-quality image after decryption even though some additional information is still contained in the image. It is further helpful to perfectly restore the original image by extracting the information if needed. Hence, RDH methods for encrypted images have been studied [5–10]. By using those methods, the payload embedded in the encrypted domain can be extracted from the decrypted image. Conversely, in the case that a payload is embedded in the plain domain and can be extracted from the encrypted image, image retrieval in the encrypted domain can be attained. Those integration methods of reversible data hiding and encryption consequently give three kinds of

user authority: (i) decryption only, (ii) data extraction only, and (iii) both decryption and data extraction. Further, if two different payloads are embedded in the plain and encrypted domains independently and could be extracted from either domain, the use of the application can be further extended. For instance, we assume that some images are preliminarily encrypted by the owner and then the encrypted images are outsourced to a third party. The owner would also like the encrypted images to be searchable without decryption. In such a scenario, it would be helpful if the owner could embed the image information such as the ownership and image content in the plain domain while the third party could embed additional information, e.g., the server information and time stamps, in the encrypted domain. We propose a flexible RDH method in both a single domain and two domains.

Zhang [5] proposed an RDH method in the encrypted domain. This method encrypts the whole image pixel-by-pixel using the exclusive-or operation and thus cannot compress the encrypted image containing a payload (hereafter, output image). The RDH process cannot be performed in two domains. Additionally, the payload may not be correctly extracted, leading to the original image not being retrieved. Hong et al. [6] modified Zhang’s method [5], but nevertheless the payload cannot be perfectly extracted and both the compression efficiency and two-domain data hiding are not considered. In Xiong et al.’s method [7], integer wavelet transform is introduced before encryption to attain a higher embedding rate and higher PSNR with the same amount of payload. It has been confirmed that this method can extract the payload and restore the original image perfectly under certain conditions. The reversibility is not ensured under different conditions. Moreover, this method does not consider compression of output images and cannot be applied to the two-domain data hiding. In another work [8], the quality of the marked image, which is equal to that of the decryption-only image, has been improved compared to [5]. However, if the payload amount is too large, the payload cannot be correctly extracted. Further, this method cannot compress the output images by using image coding standards, such as JPEG-LS [11] and JPEG 2000 [12], and cannot be extended to the two-domain data hiding. Ma et al.’s method [9] gives a particular user authority. While generally the original image cannot be retrieved without data extraction, this method can restore the original image after only the decryption. Zhang [10] proposed another approach that embeds a payload in the plain domain and can extract the

Manuscript received February 7, 2020.

Manuscript revised May 25, 2020.

[†]The authors is with the Graduate School of Engineering, Chiba University, Chiba-shi, 263-8522 Japan.

^{††}The authors is with the Graduate School of Science and Engineering, Chiba University, Chiba-shi, 263-8522 Japan.

^{†††}The author is with the Faculty of System Design, Tokyo Metropolitan University, Hino-shi, 191-0065 Japan.

a) E-mail: imaizumi@chiba-u.jp

b) E-mail: kiya@sd.tmu.ac.jp

DOI: 10.1587/transfun.2020SMP0029

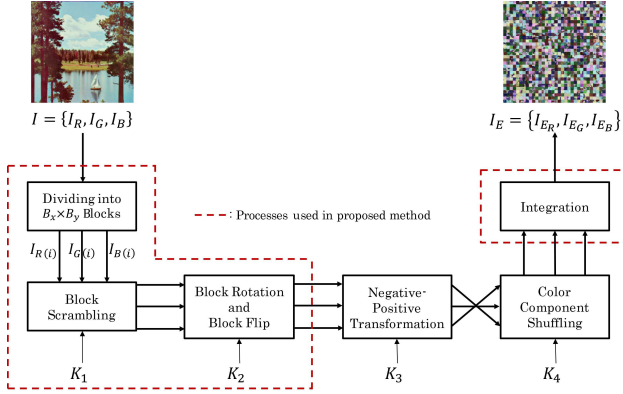


Fig. 1 Compressible encryption method for EtC system.

payload from the encrypted image. In this method, we may also embed a payload in the encrypted domain and extract the payload from the decrypted image. In those methods [9, 10], however, both the compression of the output images and the two-domain data hiding cannot be achieved.

In this paper, we propose a flexible RDH method in both a single domain and two domains. The proposed method embeds a payload in the encrypted domain and can extract the payload from the decrypted image. Conversely, this method can embed a payload in the plain domain and extract the payload from the encrypted image. Furthermore, the RDH method can be extended to both the plain and encrypted domains in our method. This extension contributes to expanding the types of user authorities. We adopt the compressible encryption (CE) method [17–20] for high compression efficiency of the output image. Additionally, the RDH method based on histogram shift (HS) [2] is introduced in our method to embed a payload in both the plain and encrypted domains and flexibly extract the payload in either domain. In the proposed method, complex conditions need to be configured to define the data hiding order and the target blocks for encryption. Those conditions enable complete data extraction without any loss of the payload. Through our experiments, we confirm the effectiveness of the proposed method in terms of lossless compression performance using JPEG-LS and JPEG 2000, data hiding capacity/marked-image quality, and robustness against ciphertext-only attacks (COAs).

2. Preparation

2.1 Compressible encryption method

Innovative frameworks for secure image transmission were proposed for encryption-then-compression (EtC) systems [13–20]. In the systems, encryption is performed by an image owner before compression/transmission. Common-key cryptosystems are frequently used for protecting visual information on plain images. However, most of those methods do not support lossless compression of the encrypted images. The CE method has been developed for a solution to this issue [17–20]. The images encrypted by using this

method are called EtC images. We introduce the CE method to our proposed method as an encryption algorithm.

The block diagram of the CE method is shown in Fig. 1. We describe the detailed procedure as follows.

- Step 1:** Divide the original image $I = \{I_R, I_G, I_B\}$ with $M \times N$ pixels into multiple blocks with $B_x \times B_y$ pixels.
- Step 2:** Scramble the position of each block using a random number generated by key K_1 .
- Step 3:** Rotate and flip each block using a random number generated by key K_2 .
- Step 4:** Perform the negative-positive transformation on each block using a random number generated by key K_3 .
- Step 5:** Shuffle the R, G, and B components in each block using a random number generated by key K_4 .
- Step 6:** Integrate all blocks and generate the encrypted image.

It is noted that the keys K_1 , K_2 , and K_3 are commonly used among the three color components in the fundamental CE method [17]. In another study, those keys are independently used among the three color components in the CE method [18]. In the case above, each key is divided into three elemental keys, such as $K_1 = \{K_{1,R}, K_{1,G}, K_{1,B}\}$. Each color component is consequently encrypted by a different key. The proposed method can adopt either case.

The first two permutation processes in the CE method, which are described in Steps 2 and 3, do not transform the image histogram. We focus on this feature and introduce these processes to our encryption algorithm.

2.2 Reversible data hiding method based on histogram shift [2]

Ni et al. proposed an RDH method for grayscale images, where the quality of the marked image can be maintained by slightly shifting the image histogram [2]. Figure 2 illustrates the embedding procedure of the HS-based RDH method. We describe each step as follows.

Step 1: A pair of a peak point (hereafter, PP), which is the bin with the highest frequency of appearance, and a zero point (hereafter, ZP), which is the bin with no pixels, is explored from the image histogram. If there are multiple pairs of PP and ZP , we should take the pair that has the shortest distance between the PP and ZP .

Step 2: We assume that X is the pixel value of pixel x_X , where x_X is a pixel in grayscale image I_g . If X is located between the PP and ZP , it is shifted according to the following equation.

$$X' = \begin{cases} X + 1, & X \in (PP, ZP) \text{ if } PP < ZP \\ X - 1, & X \in (ZP, PP) \text{ if } PP > ZP, \end{cases} \quad (1)$$

where X' denotes the pixel value after shifting. The shifted pixel is depicted as $x_{X'}$. Accordingly, the adjacent bin of PP becomes empty.

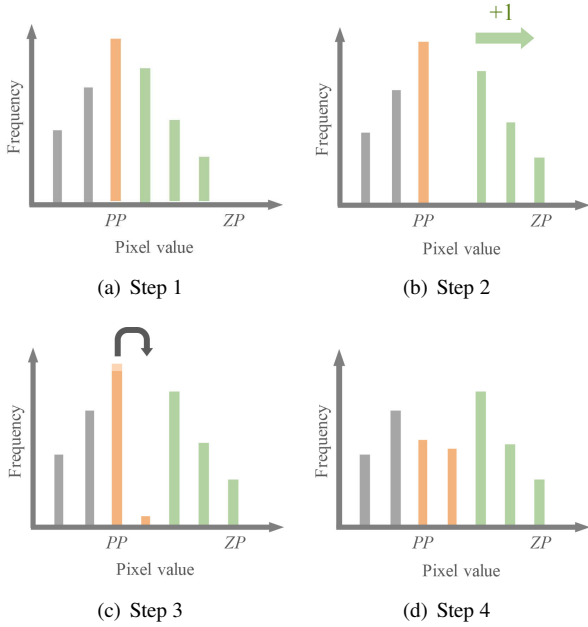


Fig. 2 Procedure of HS-based RDH.

Step 3: The payload is embedded into pixels x_{PP} . If the to-be-embedded bit is 1, the pixel value PP is shifted to the empty bin as follows:

$$PP' = \begin{cases} PP + 1 & \text{if } PP < ZP \\ PP - 1 & \text{if } PP > ZP, \end{cases} \quad (2)$$

where PP' is the marked pixel value. In contrast, if the to-be-embedded bit is 0, the pixel value is unchanged, that is,

$$PP' = PP. \quad (3)$$

Consequently, x_{PP} turns into marked pixel $x_{PP'}$.

Step 4: Step 3 is repeated until the whole of the payload is completely embedded.

In this method, the data hiding capacity is equal to the total number of pixel x_{PP} s. The capacity is increased when the number of x_{PP} s is large. If the number of x_{PP} s is less than the payload amount, the above steps are repeatedly performed until the whole of the payload is completely embedded. Therefore, a certain bin might be used as the PP more than once. Note that it is necessary to store the PP and ZP values as side information. Those values are generally embedded into the LSBs of the selected pixels. If there is no ZP in the histogram, we adopt the lowest point (LP), which is the bin with the lowest frequency of appearance. In that case, the original pixels with the LP should be recorded, and this information is embedded with the pure payload to perfectly retrieve the original image. For data extraction, we perform the above procedure in the opposite order.

3. Proposed method

We elaborate our proposed framework to embed a payload in the encrypted domain and extract the payload from the decrypted image. The proposed method can also embed a payload in the plain domain and extract the payload from the encrypted domain. Hereafter, we describe the proposed algorithm for the latter case, but it is easy to apply the procedure to the former case by interchanging the steps for encryption and data hiding. We first specify the data hiding/encryption processes with the detailed conditions and then delineate the data extraction. Subsequently, an extended framework, where two different payloads can be embedded in both the plain and encrypted domains independently, is described.

3.1 Overview of proposed method

(A) Embedded in plain domain

Figure 3 shows the block diagram of the proposed method with data hiding in a single domain. In the proposed method, we use the two permutation processes of the CE method illustrated in Fig. 1, namely, position scrambling and block rotation/flip. The other two processes, that is, negative-positive transformation and color component shuffling, are omitted to ensure the reversibility of our algorithm. Here, we describe the whole procedure including HS-based RDH and CE.

Step 1: Explore the PP and ZP in the histogram of original image I .

Step 2: Obtain the intermediate image I' by shifting the histogram between the PP and ZP . The shifted pixel values X' are given by Eq. (1).

Step 3: Divide the image I' into multiple blocks with $b_x \times b_y$ pixels, and define the a -th block containing x_{PP} as $B_{x_{PP}}(a)$.

Step 4: Determine the data hiding order within each block $B_{x_{PP}}(a)$ (details in 3.1.1).

Step 5: Determine the data hiding order among the blocks $B_{x_{PP}}(a)$ (details in 3.1.2).

Step 6: Determine the target blocks B_r for block rotation and block flip out of all the blocks (details in 3.1.3).

Step 7: Determine the target blocks B_p for position scrambling out of all the blocks (details in 3.1.4).

Step 8: Embed a payload into the pixels x_{PP} in the data hiding order defined in Steps 4 and 5. The marked pixel values PP' are given by Eqs. (2) and (3).

Step 9: Rotate and flip each block B_r .

Step 10: Scramble the position of the blocks B_p .

Step 11: By concatenating all the blocks, obtain the output image I'_E .

(B) Embedded in encrypted domain

In the case that the payload is embedded in the encrypted domain, the CE process of Steps 9 and 10 is performed

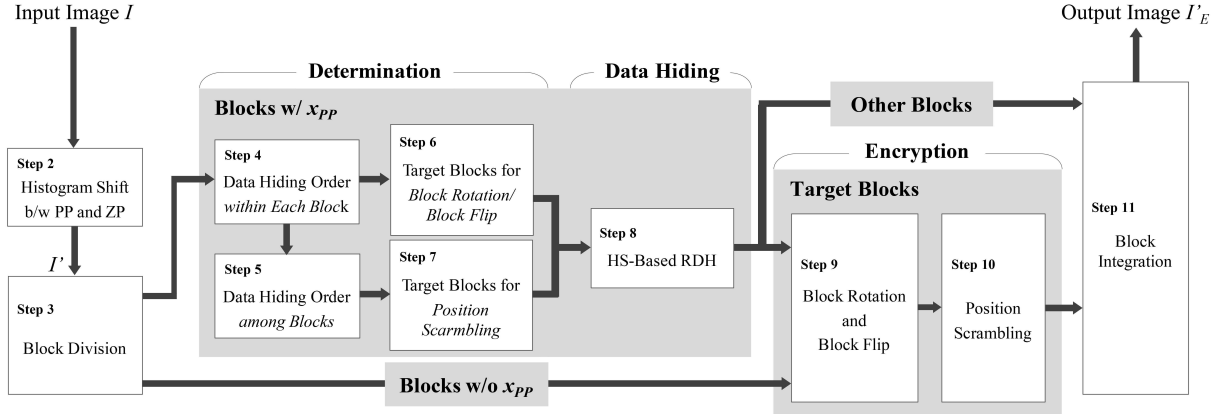


Fig. 3 Procedure of proposed method, where payload is embedded in plain domain.

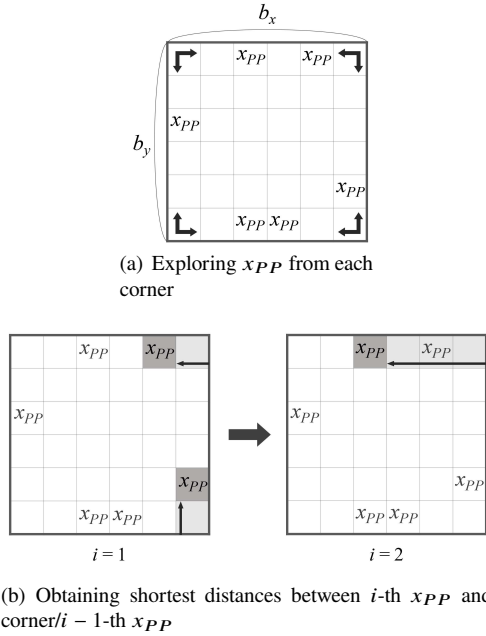


Fig. 4 Determination of data hiding order within each block.

previously. Then, the payload is embedded into the EtC image by Step 8. Finally, the output image I'_E is obtained in Step 11. Hereafter, we elaborate the conditions for the data hiding order and the target blocks for CE.

3.1.1 Data hiding order within each block

Here, we detail how to determine the data hiding order within each block in Step 4 of 3.1. The data hiding order in each block is basically equal to the raster scan order. However, we need to consider the block rotation process in encryption for perfect data extraction. We assume that the block $B_{x_{PP}}(a)$ contains N of the pixels x_{PP} . The detailed procedure to

define the order is described as follows.

- (1) Set $i = 1$.
- (2) Explore the i -th x_{PP} ($i \in [1, N]$) from each corner in the block $B_{x_{PP}}(a)$, as shown in Fig. 4(a), and record the distances between each corner and x_{PP} .
- (3) Set the corner with the shortest distance to the i -th x_{PP} as the origin/direction of the raster scan for data hiding into x_{PP} .
- (4) As shown in Fig. 4(b), if there are multiple corners/directions with the shortest distance, i is increased by 1, namely $i = i + 1$, and go back to (2). In that case, the distances between the $i - 1$ -th and i -th x_{PP} s should be recorded.
- (5) If there are still multiple corners/directions with the shortest distance in the case of $i = N$, the left-top corner and left-to-right direction are chosen as the origin and scanning direction.

3.1.2 Data hiding order among blocks

The data hiding order among the blocks $B_{x_{PP}}(a)$ in Step 5 of 3.1 is defined according to the following steps.

- (1) Sort the data hiding blocks in descending order of the number of x_{PP} s in each block.
- (2) For the blocks with the same number of x_{PP} s, sort the data hiding blocks in ascending order of the number of pixels between the PP and ZP in each block.
- (3) For the blocks with the same number of pixels between the PP and ZP , obtain the shortest distance between the origin of the data hiding order within the block and the j -th x_{PP} (set $j = 1, j \in [1, N]$). Sort the data hiding blocks in ascending order of the shortest distance. If there are multiple blocks with the same distance, j is increased by 1, namely $j = j + 1$, and repeat this step. In that case, the distances between the $j - 1$ -th and j -th x_{PP} s should be compared.
- (4) For the blocks with the same distance in (3), sort the data hiding blocks in ascending order of a .

3.1.3 Target blocks for block rotation and flip process

If the encryption processes are performed on all blocks in the image, the payload cannot be extracted correctly. We need to determine the target blocks for encryption based on several conditions. In Step 6 of 3.1, the target blocks for the rotation and flip process must satisfy either of the following conditions.

- (a) Blocks $B_{x_{PP}}$, where the data hiding order is determined by (1) – (4) of 3.1.1.
- (b) Blocks that do not contain x_{PP} .

The blocks $B_{x_{PP}}$, where the data hiding order is determined by (5) of 3.1.1, are excluded from the target blocks for the rotation and flip process.

3.1.4 Target blocks for position scrambling process

In a similar fashion, the target blocks for the position scrambling process must satisfy either of the following conditions in Step 7 of 3.1.

- (a) Blocks $B_{x_{PP}}$, where the data hiding order is determined by (1) – (3) of 3.1.2.
- (b) Blocks that do not contain x_{PP} .

The blocks $B_{x_{PP}}$, where the data hiding order is determined by (4) of 3.1.2, are excluded from the target blocks for the position scrambling process.

3.2 Data extraction

The payload embedded in 3.1 can be extracted from the output image I'_E without decryption. After the block division of I'_E and the definition of the data extracting order, the payload bits are extracted from the marked blocks in series. The detailed procedure is explained as follows.

Step 1: Divide the image I'_E into blocks, and define the α -th block containing marked pixel $x_{PP'}$ as $B_{x_{PP'}}(\alpha)$.

For all the blocks $B_{x_{PP'}}(\alpha)$,

Step 2: Determine the data extracting order within each block according to the conditions described in 3.1.1.

Step 3: Determine the data extracting order among the blocks according to the conditions described in 3.1.2.

Step 4: According to the data hiding order defined in Steps 2 and 3, extract the payload from $x_{PP'}$. The original pixels x_{PP} are retrieved as follows. If the embedded bit is 1, the marked pixel value PP' is shifted as

$$PP = \begin{cases} PP' - 1 & \text{if } PP < ZP \\ PP' + 1 & \text{if } PP > ZP. \end{cases} \quad (4)$$

If the embedded bit is 0, the pixel is unchanged, that is,

$$PP = PP'. \quad (5)$$

For all the blocks,

Step 5: By concatenating all the blocks and shifting the histogram between the PP and ZP according to the following equation, obtain the EtC image I_E without the payload.

$$X = \begin{cases} X' - 1, & X' \in (PP + 1, ZP + 1) \text{ if } PP < ZP \\ X' + 1, & X' \in (ZP - 1, PP - 1) \text{ if } PP > ZP. \end{cases} \quad (6)$$

In accordance with the above procedure, the payload embedded in the plain domain can be perfectly extracted from the EtC image. When the EtC image I_E is decrypted, the original image is retrieved completely. In this way, the proposed method can flexibly extract the payload and decrypt the EtC image without regard to the order of extraction and decryption. This is due to the invariance of the image histogram before/after encryption. Consequently, the receiver types can be classified into three cases: extraction only, decryption only, and both extraction and decryption.

In the case that the payload embedded into the EtC image is extracted from the decrypted image, the output image I'_E is first decrypted based on the conditions defined in 3.1.3 and 3.1.4. Then, the payload is extracted according to the extracting order (Steps 1 – 4). Finally, the original image is retrieved by Step 5.

3.3 Data hiding in two domains

Here, we extend the proposed method to embed two different payloads in the plain and encrypted domains independently. Figure 5 shows the block diagram of the extended framework. In this framework, we divide the original image into two regions beforehand. Then, while one of the payloads is embedded into one region before encryption, the other payload can be embedded into the other region. We elaborate the procedure of this extension in the following steps.

Step 1: Explore the PP and ZP in the histogram of the original image I .

Step 2: Obtain the intermediate image I' by shifting the histogram between the PP and ZP . The shifted pixel values X' are given by Eq. (1).

Step 3: Divide the image I' into multiple blocks with $b_x \times b_y$ pixels.

Step 4: Prepare two regions A and B , and assign each block to either A or B using a pseudo-random sequence. The α -th block containing x_{PP} assigned into A and the β -th block containing x_{PP} assigned into B are represented as $B_{x_{PP},A}(\alpha)$ and $B_{x_{PP},B}(\beta)$, respectively.

For the blocks $B_{x_{PP},A}(\alpha)$,

Step 5A: Determine the data hiding order and the target blocks for encryption according to Steps 4 – 7 in 3.1.

Step 6A: Embed a payload into the pixels x_{PP} in sequence. The marked pixel values PP' are given by Eqs. (2) and (3).

Step 7A: Perform encryption for the target blocks.

Step 8A: Obtain the output region A'_E .

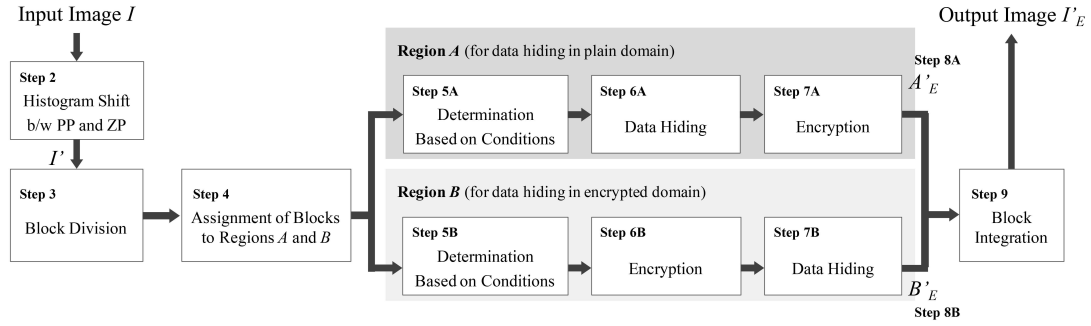


Fig. 5 Extended framework for data hiding in two domains.

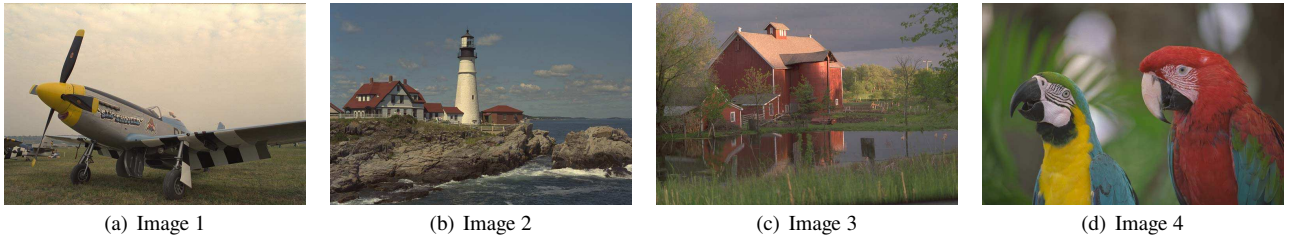


Fig. 6 Test images.

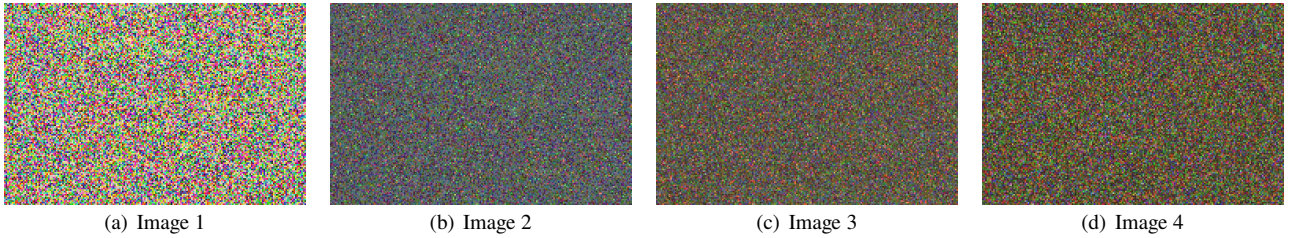


Fig. 7 Output images by single-domain data hiding method (block size: 16×16 pixels).

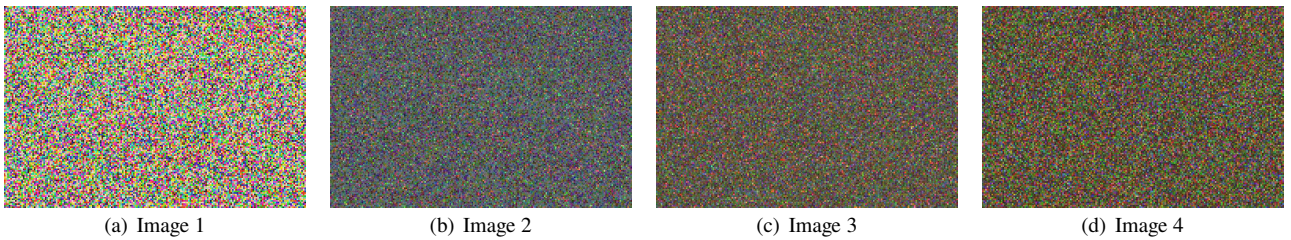


Fig. 8 Output images by two-domain data hiding method (block size: 16×16 pixels).

Similarly, for the blocks $B_{x_{PP},B}(\beta)$,

Step 5B: Determine the data hiding order and the target blocks for encryption according to Steps 4 – 7 in 3.1.

Step 6B: Perform encryption for the target blocks.

Step 7B: Embed another payload into the pixels x_{PP} in sequence. The marked pixel values PP' are given by Eqs. (2) and (3).

Step 8B: Obtain the output region B'_E .

Finally,

Step 9: By concatenating the regions A'_E and B'_E , obtain the output image I'_E .

In this framework, the two independent regions are derived before the main processes. Accordingly, the types of

user authorities can be extended, e.g., data extraction in region A only and data extraction in region B with decryption.

4. Experimental results

We specify the effectiveness of the proposed method from the aspects of lossless compression performance using JPEG-LS [11] and JPEG 2000 [12], hiding capacity/image quality, and robustness against COAs. The four $2,048 \times 3,072$ images [21] shown in Fig. 6 were used as test images. The block size in our experiments is 16×16 pixels. We tested 20 times for each image, namely, we generated 20 output images each. Pseudo-random number sequences are used as the payload, and the payload amount is equal to the data hiding capacity. Figure 7 shows the output images obtained by the proposed method with data hiding in a single domain. Similarly, Fig. 8 depicts the output images by the extended proposed method for data hiding in two domains, as described in 3.3. The output images obtained by those two methods are quite similar to each other. In this experiment, we adopt the independent CE processing of RGB components [18] in the encryption process.

4.1 Compression performance

We evaluate the lossless compression performance using JPEG-LS and JPEG 2000. Figures 9 and 10 show the compression ratio of the original and output images, where the block size is 16×16 , 32×32 , or 64×64 pixels. Those values are the average of the compression ratio for 20 output images. It is confirmed that the output images by the proposed methods can be greatly compressed while those obtained by the pixel-based encryption method [5] cannot be compressed at all. According to Fig. 9, the original and output images show quite analogous results in JPEG-LS compression. In contrast, the CE process marginally affects the compression ratio of the output images using JPEG 2000, as shown in Fig. 10. This is because a discrete wavelet transform in the JPEG 2000 coding system uses the correlation calculated from the wider spatial range of an image than JPEG-LS. In our methods, the compression performance is better when the block size is larger.

4.2 Data hiding capacity and image quality

The data hiding capacity and the marked-image quality of the proposed methods are compared with those of Zhang's method [5]. The marked image means the decryption-only image here. Table 1 shows the comparison results. The proposed methods are superior to Zhang's method in both the capacity and the image quality. In Zhang's method, one bit is embedded into each divided block, and thus the hiding capacity depends on the block size. In this experiment, the block size in Zhang's method is set as 16×16 pixels. If the block size is smaller than 16×16 pixels, the data hiding capacity increases, but the extracted-bit error rate becomes higher. Even when the block size is 16×16 pixels, the

payload cannot be extracted correctly in those test images. Additionally, the lower three bits are flipped in half of all the pixels statistically, and thus the total number of flipped bits directly affects the marked-image quality. In contrast, in the proposed methods, both the data hiding capacity and the marked-image quality are constant irrespective of block size.

4.3 Robustness against ciphertext-only attacks

Here, we consider robustness against COAs, where an attacker is assumed to have access only to ciphertexts. Our CE method is based on the premise that encryption keys are securely maintained, and the CE method prepares different encryption keys for each image/user. Brute force attacks and jigsaw puzzle solver (JPS) attacks are cited as COAs for the CE method. The robustness against those two types of attacks has already been evaluated in our previous works such as [17–19, 22, 23]. The robustness does not deteriorate even when a CE image contains a payload. JPS attacks prompt the assembly of a jigsaw puzzle by using the correlation among pieces. We regard blocks of a CE image as pieces of a jigsaw puzzle. Although the robustness against JPS attacks has been revealed by our previous works, we purposely compute the correlation coefficient [24] to confirm a part of the correlation among blocks. The correlation coefficient has been used in multiple literatures [25, 26] for security analysis.

The output image is encrypted block by block, and thus the correlation among the neighboring blocks is calculated. In EtC images, the correlation among pixels within each block is retained for high-performance compression. As shown in Fig. 11, we derived the resized images of the original and output images by taking the top-left pixels from each block, where the image size is reduced to 128×198 pixels.

The 2,000 pairs of the neighboring pixels are randomly chosen in horizontal, vertical, and diagonal directions. Then, the correlation coefficients are calculated for each direction. The correlation coefficient $r_{x,y}$ between the two neighboring pixels x and y is given as

$$r_{x,y} = \frac{cov(x,y)}{\sqrt{D(x)}\sqrt{D(y)}}, \quad (7)$$

where $D(x)$, $D(y)$, and $cov(x,y)$ are represented as

$$D(x) = \frac{1}{S} \sum_{j=1}^S (x_j - E(x))^2, \quad (8)$$

$$D(y) = \frac{1}{S} \sum_{j=1}^S (y_j - E(y))^2, \quad (9)$$

$$cov(x,y) = \frac{1}{S} \sum_{j=1}^S (x_j - E(x))(y_j - E(y)). \quad (10)$$

Here, S represents the number of neighboring-pixel pairs ($S = 2,000$ in this experiment), and $E(x)$ and $E(y)$ are the average of the pixels x_i and y_i , which are shown as

$$E(x) = \frac{1}{S} \sum_{j=1}^S x_j, \quad (11)$$

$$E(y) = \frac{1}{S} \sum_{j=1}^S y_j. \quad (12)$$

Table 2 shows the correlation coefficients $r_{x,y}$ for the original

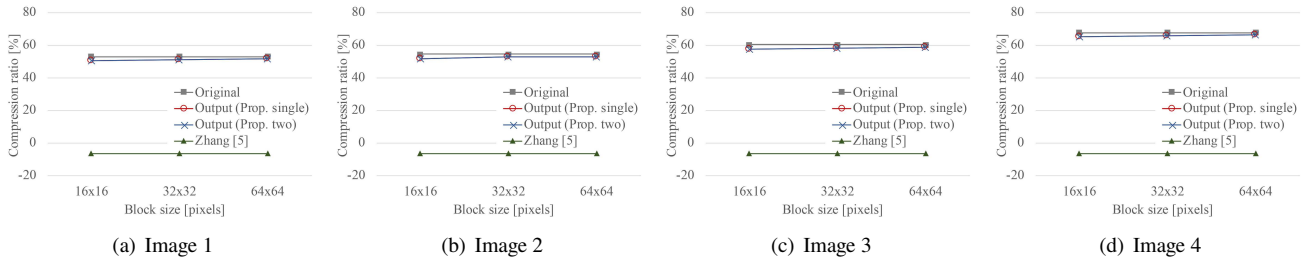


Fig. 9 Lossless compression performance using JPEG-LS.

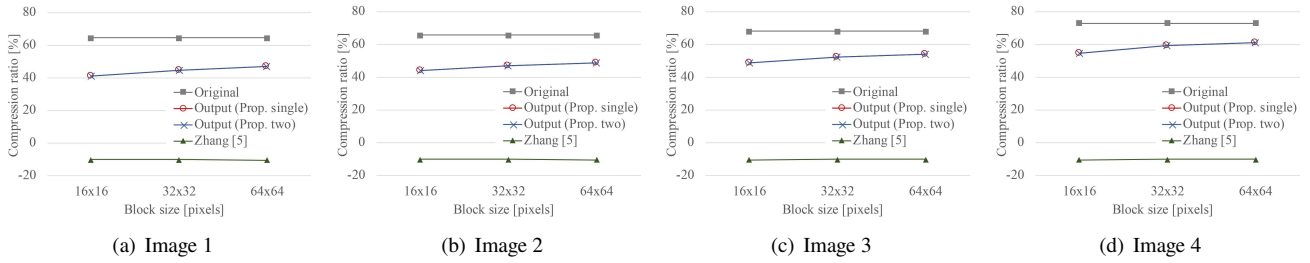


Fig. 10 Lossless compression performance using JPEG 2000.

Table 1 Data hiding capacity and marked-image quality

Method	Image 1		Image 2		Image 3		Image 4	
	Capacity [bits]	PSNR [dB]	Capacity [bits]	PSNR [dB]	Capacity [bits]	PSNR [dB]	Capacity [bits]	PSNR [dB]
Prop. single	313,482	57.44	601,220	52.56	484,534	52.00	528,158	54.55
Prop. two	313,482	57.44	601,220	52.56	484,534	52.00	528,158	54.55
Zhang [5]	73,728	41.52	73,728	41.50	73,728	41.49	73,728	41.50

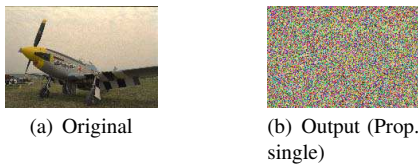


Fig. 11 Resized images.

Table 2 Correlation coefficients between neighboring pixels in resized image.

		Horizontal	Vertical	Diagonal
Image 1	Original	0.9776	0.9539	0.9432
	Output (Prop. single)	-0.0024	0.0012	0.0010
	Output (Prop. two)	-0.0077	0.0009	-0.0003
Image 2	Original	0.8186	0.7534	0.7110
	Output (Prop. single)	-0.0017	-0.0024	-0.0013
	Output (Prop. two)	0.0002	0.0014	0.0051
Image 3	Original	0.8221	0.8953	0.8348
	Output (Prop. single)	-0.0016	-0.0025	-0.0010
	Output (Prop. two)	-0.0022	-0.0058	0.0077
Image 4	Original	0.9378	0.9366	0.9298
	Output (Prop. single)	0.0016	-0.0010	0.0015
	Output (Prop. two)	-0.0260	0.0049	0.0016

and output images. Those values are the average of $r_{x,y}$ for

20 output images. It is verified that the $r_{x,y}$ values of the output images are close to 0, and thus the correlation among blocks is quite low.

5. Conclusions

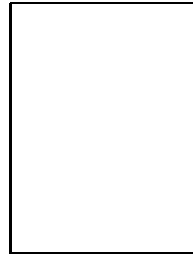
We proposed an effective RDH method that embeds a payload in the encrypted domain and can directly extract the payload from the decrypted image. In an opposite fashion, the proposed method can also embed a payload in the plain domain and extract the payload from the encrypted image. Namely, we can choose either the plain or encrypted domain for data hiding. The compressible encryption method for the EtC system is adopted in the proposed method, and the HS-based RDH method is integrated into our framework. We further extended the proposed method to embed a payload in the plain and encrypted domains. The output images obtained by the proposed methods have been evaluated in terms of lossless compression performance by JPEG-LS and JPEG 2000, data hiding capacity/marked-image quality, and correlation among blocks. Our new method can provide an efficient framework to flexibly integrate both encryption and data hiding techniques.

Acknowledgement

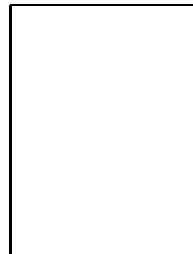
This work was partially supported by Grant-in-Aid for Research Activity start-up, No.19K23070, from the Japan Society for the Promotion Science.

References

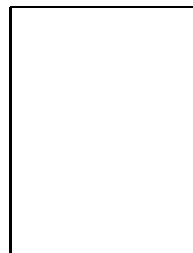
- [1] Y. Q. Shi, X. Li, X. Zhang, H. T. Wu, B. Ma, "Reversible data hiding: Advances in the past two decades," *IEEE Access.*, vol.4, pp.3210-3237, 2016.
- [2] Z. Ni, Y. -Q. Shi, N. Ansari, W. Su, "Reversible data hiding," *IEEE Trans. Circ. Syst. Vid. Tech.*, vol.16, no.3, pp.354-362, 2006.
- [3] D. M. Thodi, J. J. Rodriguez, "Expansion Embedding Techniques for Reversible Watermarking," *IEEE Trans. Image Process.*, vol.16, no.3, pp.721-730, 2007.
- [4] M. Fujiyoshi, S. Sato, H. L. Jin, and H. Kiya, "A location-map free reversible data hiding method using block-based single parameter," *Proc. IEEE ICIP*, vol.III, pp.257-260, 2007.
- [5] X. Zhang, "Reversible data hiding in encrypted image," *IEEE Signal Process. Lett.*, vol.18, no.4, pp.255-258, 2011.
- [6] W. Hong, T. S. Chen, and H. Y. Wu, "An improved reversible data hiding in encrypted images using side match," *IEEE Signal Process. Lett.*, vol.19, no.4, pp.199-202, 2012.
- [7] L. Xiong, Z. Xu, and Y. Q. Shi, "An integer wavelet transform based scheme for reversible data hiding in encrypted images," *Multidimensional Syst. Signal Process.*, vol.29, no.3, pp.1191-1202, 2018.
- [8] X. Zhang, "Separable reversible data hiding in encrypted image," *IEEE Trans. Inf. Forensics Security*, vol.7, no.2, pp.826-832, 2012.
- [9] K. Ma, W. Zhang, X. Zhao, N. Yu, and F. Li, "Reversible data hiding in encrypted images by reserving room before encryption," *IEEE Trans. Inf. Forensics Security*, vol.8, no.3, pp.553-562, 2013.
- [10] X. Zhang, "Commutative reversible data hiding and encryption," *Secur. Commun. Netw.*, vol.6, no.11, pp.1396-1403, 2013.
- [11] M. J. Weinberger, G. Seroussi, and G. Sapiro, "The LOCO-I lossless image compression algorithm: principles and standardization into JPEG-LS," *IEEE Trans. Image Process.*, vol.9, no.8, pp.1309-1324, 2000.
- [12] "Information technology - JPEG 2000 image coding system - Part 1: Core coding system," *International Standard ISO/IEC IS-15444-1*, Dec. 2000.
- [13] M. Kumar and A. Vaish, "An efficient encryption-then-compression technique for encrypted images using SVD," *Digital Signal Processing*, vol.60, pp.81-89, 2017.
- [14] J. Zhou, X. Liu, O.C. Au, and Y.Y. Tang, "Designing an efficient image encryption-then-compression system via prediction error clustering and random permutation," *IEEE Trans. Information Forensics and Security*, vol.9, no.1, pp.39-50, 2014.
- [15] W. Liu, W. Zeng, L. Dong, and Q. Yao, "Efficient compression of encrypted gray-scale images," *IEEE Trans. Image Process.*, vol.19, no.4, pp.1097-1102, 2010.
- [16] M. Johnson, P. Ishwar, V. Prabhakaran, D. Schinberg, and K. Ramchandran, "On compressing encrypted data," *IEEE Trans. Signal Process.*, vol.52, no.10, pp.2992-3006, 2004.
- [17] K. Kurihara, M. Kikuchi, S. Imaizumi, S. Shiota, and H. Kiya, "An encryption-then-compression system for JPEG/Motion JPEG standard," *IEICE Trans. Fundamentals*, vol.E98-A, no.11, pp.2238-2245, 2015.
- [18] S. Imaizumi and H. Kiya, "A block-permutation-based encryption scheme with independent processing of RGB components," *IEICE Trans. Inf. & Sys.*, vol.E101-D, no.12, pp.3150-3157, 2018.
- [19] K. Kurihara, S. Imaizumi, S. Shiota, and H. Kiya, "An encryption-then-compression system for lossless image compression standards," *IEICE Trans. Inf. & Sys.*, vol.E100-D, no.1, pp.52-56, 2017.
- [20] O. Watanabe, A. Uchida, T. Fukuhara, and H. Kiya, "An encryption-then-compression system for JPEG 2000 standard," in *Proc. on IEEE ICASSP*, pp.1226-1230, 2015.
- [21] [Online] Available: https://www.math.purdue.edu/~lucier/PHOTO_CD/D65_TIFF_IMAGES/
- [22] T. Chuman, K. Kurihara, and H. Kiya, "On the security of block scrambling-based EtC systems against extended jigsaw puzzle solver attacks," *IEICE Trans. Inf. & Sys.*, vol.E101-D, no.1, pp.37-44, 2018.
- [23] W. Sirichotedumrong and H. Kiya, "Grayscale-based block scrambling image encryption using YCbCr color space for encryption-then-compression systems," *APSIPA Trans. Signal Inform. Process.*, e7, vol.8, 2019.
- [24] A. G. Bluman, "Elementary statistics: A step by step approach," Tenth ed., McGraw-Hill, 2018.
- [25] C. K. Huang and H. H. Nien, "Multi chaotic systems based pixel shuffle for image encryption," *Optics Communications*, vol.282, no.11, pp.2123-2127, 2009.
- [26] A. Belazi, A. A. Abd El-Latif, and S. Belghith, "A novel image encryption scheme based on substitution-permutation network and chaos," *Signal Process.*, vol.128, pp.155-170, 2016.



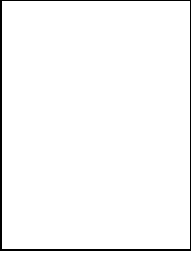
Shoko IMAIZUMI received her B. Eng., M. Eng., and Ph.D. degrees from Tokyo Metropolitan University, Japan in 2002, 2005, and 2011. In 2011, she joined Chiba University, where she is currently an Associate Professor of the Graduate School of Engineering. From 2003 to 2004, she was with the Ministry of Education, Culture, Sports, Science and Technology of Japan. She was a Researcher at the Industrial Research Institute of Niigata Prefecture from 2005 to 2011. Her research interests include image processing and multimedia security. She served as an Associate Editor for *IEICE Trans. Fundamentals* in 2016-2020, and is currently a Director for SPIJ (Society of Photography and Imaging of Japan). She is a member of IEICE, ITE, IEEE, SPIJ, IEEE, and APSIPA.



Yusuke IZAWA received his B. Eng. and M. Eng. degrees from Chiba University, Japan in 2018 and 2020. He joined the National Printing Bureau in 2020. His research interests include multimedia security.



Ryoichi HIRASAWA received his B.Eng. degree from Chiba University, Japan in 2019. Since 2019, he has been a Master course student at Chiba University. His research interests include image processing.



Hitoshi KIYA received his B.E. and M.E. degrees from Nagaoka University of Technology, Japan in 1980 and 1982 and his Dr. Eng. degree from Tokyo Metropolitan University in 1987. In 1982, he joined Tokyo Metropolitan University, where he became Full Professor in 2000. From 1995 to 1996, he attended the University of Sydney, Australia, as a Visiting Fellow. He is a Fellow of IEEE, IEICE, and ITE. He currently serves as President of APSIPA, and he served as Inaugural Vice President (Technical Activities)

of APSIPA in 2009-2013 and as Regional Director-at-Large for Region 10 of the IEEE Signal Processing Society in 2016-2017. He was also President of the IEICE Engineering Sciences Society in 2011-2012, and he served there as Vice President and Editor-in-Chief for the IEICE Society Magazine and Society Publications. He has been an Editorial Board Member of eight journals, including IEEE Trans. on Signal Processing, Image Processing, and Information Forensics and Security, Chair of two technical committees, and Member of nine technical committees including the APSIPA Image, Video, and Multimedia Technical Committee (TC) and IEEE Information Forensics and Security TC. He has organized a lot of international conferences in such roles as TPC Chair of IEEE ICASSP 2012 and as General Co-Chair of IEEE ISCAS 2019. Dr. Kiya has received numerous awards, including ten best paper awards.